DOE/ET-53088-308 IFSR #308

Radial Fluctuation Scale of Ion Temperature Gradient Driven Turbulence

P.W. Terry, J.N. Leboeuf,[a] *P.H. Diamond,*[b] *D.R. Thayer,*[c]
J.E. Sedlak, and *G.S. Lee*[a]

Institute for Fusion Studies
The University of Texas at Austin
Austin, Texas 78712

[a] Oak Ridge National Laboratory, Oak Ridge, TN
[b] UCSD, La Jolla, CA
[c] Lawrence Berkeley Lab., Berkeley, CA

January 1988

Radial Fluctuation Scale of Ion Temperature Gradient Driven Turbulence

P.W. Terry[a], J.N. Leboeuf [b],P.H. Diamond[c],
D.R. Thayer[d], J.E. Sedlak[a], and G.S. Lee [b]

[a]*Institute for Fusion Studies, University of Texas at Austin, Austin, Texas 78712*
[b]*Oak Ridge National Laboratory, Oak Ridge, Tennessee 37830*
[c]*Physics Dept., University of California at San Diego, La Jolla, California 92093*
[d]*Lawerence Berkeley Laboratory, University of California at Berkeley, Berkeley, California 94720*

We show that ion temperature gradient driven turbulence supports fluctuations with broader radial scales than those inferred previously on the basis of the eigenfunction with lowest radial eigenmode number. These fluctuations of greater radial extent are more strongly excited and are shown to result in fluctuation levels and transport coefficients which can be considerably larger than those previously predicted. It is expected that transport of this nature would force ion temperature and density profiles to near-marginal stability in neutral beam and ICRF heated plasmas.

I. Introduction

Evidence that anomalous ion transport is an important aspect of confinement in both ohmic and auxiliary heated tokamaks has been accumulating[1-4]. In D-III, for example, departures from neoclassical ion thermal conductivity, both with regard to its radial dependence and magnitude, have been observed[1]. In Alcator C, such anomalous ion energy losses have been linked to confinement saturation in ohmic discharges, with the additional observation that in pellet injection where the density gradient steepens, ion heat conduction decreases[2]. Ion losses at confinement saturation have also been linked to fluctuations propagating in the ion diamagnetic direction and these too have been shown to decrease with density gradient steepening due to pellet injection[3]. Ion temperature gradient driven turbulence[4,5] has been quite sucessful in explaining these features. Notably, ion thermal conductivity has strong ion density gradient scaling [$\chi_i \propto \omega_* \rho_s^2 (ln (1 + \eta_i))^2 (1 + \eta_i)^2 L_n/L_s \tau^2$ where $\eta_i = d ln\, T_i / d ln\, n_i$]. This strong dependence on η_i is responsible for the sensitivity of confinement to the density profile and enforces proximity to marginal values of η_i as well. The fluctuations of ion temperature gradient driven turbulence also propagate in the ion diamagnetic direction. Moreover, theoretical conductivities have performed well in transport codes, such as those modeling discharges with auxilary heating[6].

The tendency of ion temperature gradient driven turbulence to enforce marginal profiles does not obviate the need for nonlinear theory. On the contrary, the scalings and magnitudes of the transport coefficients which ultimately determine the confinement and profiles must be found from nonlinear theory. Previous theory has assumed that the radial correlation length of turbulence is given approximately by the width of the *lowest* order (ℓ=0) radial eigenmode (ℓ is the radial eigenmode number). This assumption naturally affects the magnitude of diffusivities since the linear driving is a function of radial mode structure. Moreover, this approximation fixes the radial width over which fluctuations mix the ion pressure, and thus determines the fluctuation level consistent with a given growth rate. More subtly, restricting the characterization of turbulence to a single radial eigenmode implies that turbulent fluctuations are modeled by a single radial wavenumber for each polodial wavenumber.

From linearized fluid equations, it is easily shown that higher order radial eigenmodes are both less localized and more strongly excited than the lowest order eigenmode. Both these features tend to increase predicted fluctuation levels and transport coefficients. The larger growth rate suggests that fluctuations with broader mode widths should predominate in determining the radial fluctuation scale. In fact, this is observed in simulations of ion temperature gradient driven turbulence where broader fluctuation scales characterize the turbulence in both growing and saturated phases[7]. It should be pointed out that the simulations, which include kinetic effects (ion Landau damping) not accounted for in the fluid equations, restrict the range in eigenmode number ℓ for which there is instability. Nevertheless, numerical solution of kinetic equations shows that fluctuations with eigenmode numbers in the range $1 \leq \ell \leq \sim 10$ remain both more extended and more strongly driven than the $\ell = 0$ fluctuation. In this paper, we discuss the inclusion of broader radial fluctuation scales in the theoretical analysis of ion temperature gradient driven turbulence and present evidence from particle simulation which corroborates the theoretical assertions.

The simplest estimates of the effect of broader mode structure on fluctuation levels and diffusivities incorporate the growth rates and radial fluctuation scales of linear theory in mixing length analyses. However, there is no reason, a priori, to assume that linear eigenmode structure and growth rates typify the fluctuations and relaxation times associated with finite amplitude turbulence. To this end, an analysis of the renormalized equations of ion temperature gradient driven turbulence is presented. The natural radial fluctuation scales and turbulent diffusivities consistent with a steady state are determined by an eigenmode calculation with D, the turbulent diffusivity, as the eigenvalue[8]. It is shown that the more strongly driven, broader radial fluctuations anticipated from linear theory give rise, in the nonlinear regime, to transport coefficients which are considerably higher than those of previous theory, *typically by an order of magnitude*. The results of the nonlinear eigenmode analysis indicate that the scales characteristic of turbulent fluctuations do not strongly differ from those inferred from linear theory for higher order eigenmodes. The evidence from particle simulations supports the conclusions of theory: higher order eigenmodes dominate the radial fluctuation spectrum in the linear phase and these broader structures persist in the nonlinear phase. The scalings of linear growth rate and modewidth with respect to shear, gradient drive and mode number carry over directly into the scalings

typical of the saturated state, further supporting the notion that the presence of broader radial mode structure strongly affects fluctuation levels and transport.

Both fluid and kinetic theories are utilized in this paper. Because fluid theory is simpler and more transparent, the basic theoretical analysis will be presented using fluid equations valid for $\eta_i > \eta_{i\,cr}$. Kinetic theory is necessary in order to determine the stability threshold for higher order radial eigenmodes which, because of greater radial extent are more sensitive to ion Landau damping. As noted above, kinetic effects are found to restrict the range of unstable eignemodes to $0 \leq \ell \leq \sim 10$; the trend of enhancement of transport for fluctuations with $1 \leq \ell \leq \sim 10$ over those with $\ell = 0$ persists. The validity of fluid theory is checked by comparing mixing length diffusivities generated from fluid and kinetic theories. The two theories show close agreement for $\ell \leq 4$ with the kinetic diffusivity peaking at slightly higher values ($\ell \sim 7$) while the fluid diffusivity continues to increase.

The results of this paper are summarized by writing $\chi_i \approx C \cdot T^{3/2} B_T^{-2} (1+\eta_i)^2$, where the constant multiplier C is an order of magnitude greater when proper account of more extended radial fluctuations is taken. As already noted, ion temperature gradient driven turbulence tends to enforce marginal stability. This follows more from the strong dependence of χ_i on η_i than from the magnitude of C. However, the larger multiplier is significant because with it, the regime of marginal stability is extended toward the edge, where the tendency of cooler temperatures to lower χ_i is offset by the increased multiplier. The scaling of the multiplier with respect to L_s is also affected by more extended fluctuation structure. Assuming fluctuations with $\ell = 0$ only, $C \sim L_s^{-1}$. With the inclusion of higher order eigenmodes, C tends to increase with L_s. The organization of this paper is as follows: In Sec. II, simulation results are presented which show extended mode structure for both linearly unstable and saturated cases. Next, the basic fluid model is introduced in Sec. III, along with the linear characteristics of higher order eigenmodes. Renormalized fluid theory is then presented in Sec. IV, and the results of the numerical solution of the eigenvalue problem are given. Section IV includes mixing length estimates for the diffusivity which are calculated from both kinetic and fluid theory and compared to the results of the nonlinear calculation

II. Simulations

Particle simulations have the virtue that the type of fluctuation structure which characterizes the turbulence as determined by balances of driving, dissipation, and nonlinear transfer, is naturally selected by the physics incorporated into the simulation. Simulations thus indicate if the linear tendency to greater excitation with higher eigenmode number actually results in more extended fluctuations and increased excitation. Particle simulations of ion temperature gradient driven turbulence have been performed using a $2\frac{1}{2}$-D particle code with full ion dynamics and adiabatic electrons in a sheared slab[9]. In these simulations, unstable η_i-mode fluctuations were allowed to grow out of noise to finite amplitudes and saturate by nonlinear transfer to ion Landau damping. Two types of simulations were performed: those in which unstable fluctuations were characterized by a single poloidal wavenumber k_y, and those with multiple k_y's unstable. In both types of simulation, careful filtering in wavenumber space was used to limit the fluctuations to either even parity or odd parity with respect to the rational surface[7]. In the first case, the single mode grew linearly and saturated. Saturation was typically accompanied by strong ion temperature profile flattening (the density profile was relatively unchanged) suggesting a quasilinear relaxation process. Some cascading occured as well however, since other wavenumbers were excited nonlinearly. The radial structure of fluctuations corresponding to the unstable wavenumber was observed both before and after saturation. It was noted that radial structure in the saturated state was essentially unaltered from the linear phase. The radial fluctuation structure was noticeably broader than that predicted for the $\ell = 0$ eigenmode from linear theory. Figure 1 shows the radial structure at saturation of the even mode corresponding to $k_y\rho_s = 0.3$, $\eta_i = 4$, $L_s/L_n = 28$, and $T_e/T_i = 1$ and compares it with $\ell = 0$ and $\ell = 2$ linear eigenmode structures. It is clear that the $\ell = 2$ mode is strongly excited. It is also observed that prior to saturation, this mode grows at a rate consistent with the $\ell = 2$ growth rate and oscillates at the $\ell = 2$ frequency. Figure 2 shows the radial structure of an odd mode corresponding to $k_y\rho_s = 0.3$, $\eta_i = 10$, $L_s/L_n = 11.2$, and $T_e/T_i = 1$. Here it is apparent from the comparisons with linear eigenmodes that modes corresponding to $\ell = 1$, $\ell = 3$, and $\ell = 5$ are simultaneously excited. The measured

potential fluctuation levels at saturation yield the following scalings: $e\phi/T_e \propto L_s/L_n$ and $e\phi/T_e \propto (1+\eta_i)^{1/2}$. Irrespective of mode parity, the fluctuation level increases with decreasing shear strength and has a weaker dependence on η_i than expected. However, saturation in the simulations occurs by temperature profile flattening over the width of the highest radial eigenmode excited. This quasilinear mechanism likely has a strong effect on the scalings.

Simulation runs with unstable fluctuations corresponding to multiple poloidal wavenumbers were studied in order to verify that negative interference between fluctuations of different wavenumber could not in some way suppress higher order radial structures. Again it was found that broader structure persisted both in linear phases and nonlinear phases. It was observed in a run with $\eta_i = 10$, $L_s/L_n = 10$, and $T_e/T_i = 1$ that fluctuations of a given wavenumber were dominated by radial structure associated with a particular eigenmode number ℓ. Thus, fluctuations in the spectrum at $k_y\rho_s \cong 0.1$ had a radial structure characterized by $\ell = 5$, whereas at $k_y\rho_s \cong 0.5$, $\ell = 1$ typified the radial structure. This observation suggests that some nonlinear coupling of radial mode structures occurs. The nonlinear coupling of radial mode structure will be considered analytically in the future.

It is clear from the simulation of cases involving both a single unstable wavenumber fluctuation and those of multiple wavenumbers that broader radial fluctuation structure than that associated with the lowest order radial eigenmode characterized η_i turbulence. This fact, which is independent of the way in which saturation occurs, establishes the need for inclusion of higher order radial wavenumbers in the theory of ion temperature gradient driven turbulence.

III. Basic Equations and Linear Theory

A fluid description of ion temperature gradient driven turbulence is contained in equations for vorticity $\nabla_\perp^2\hat{\phi}$, parallel (ion) velocity $\hat{v}_{||}$, and pressure $\hat{p}$. Assuming a sheared slab geometry, these equations are

$$\frac{\partial}{\partial t}(1-\nabla_\perp^2)\hat{\phi} - \hat{b}\times\nabla\hat{\phi}\cdot\nabla_\perp(\nabla_\perp^2\hat{\phi}) + \nabla_\parallel\hat{v}_\parallel + v_D\left(1+\frac{(1+\eta_i)}{\tau}\nabla_\perp^2\right)\nabla_y\hat{\phi} = 0,$$

$$\frac{\partial}{\partial t}\hat{v}_\parallel + \hat{b}\times\nabla\hat{\phi}\cdot\nabla\hat{v}_\parallel - \mu\nabla_\parallel^2\hat{v}_\parallel = \nabla_\parallel\hat{\phi} - \nabla_\parallel\hat{p},$$

$$\frac{\partial\hat{p}}{\partial t} + v_D\frac{(1+\eta_i)}{\tau}\nabla_y\hat{\phi} + \hat{b}\times\nabla\hat{\phi}\cdot\nabla\hat{p} = -\Upsilon\nabla_\parallel\hat{v}_\parallel \qquad (1)$$

where $v_D = -(cT_e/eB)\, d\ln n/dx$ is the diamagnetic velocity, $\tau = T_e/T_i$, $\mu = \mu_\parallel \omega_{ci}/c_s^2$ is the ion viscosity, and $\Upsilon = \Gamma/\tau$ where Γ is the ratio of specific heats. The adiabatic compression term in the pressure equation $\Upsilon\nabla_\parallel\hat{v}_\parallel$ serves to exchange energy between the driven pressure fluctuations and fluctuations in the parallel velocity which experience viscous dissipation at high k through the viscosity term $\mu\nabla_\parallel^2\hat{v}_\parallel$ [4]. This term effectively plays the role of Landau damping in the fluid theory by providing dissipation at large $k_\parallel$ where ions resonate with the wave. Near the critical η_i where modes are marginally stable, kinetic effects play an important role[10,11]. Thus, the fluid model is valid only for $\eta > \eta_{i\,cr}$. It is also assumed that $L_n^2 < L_T L_s$ where L_n, L_T, and L_s are the scale lengths of density gradient, temperature gradient, and magnetic shear. The case where $L_n^2 > L_T L_s$ is the 'flat density' case which, while also amenable to fluid theory, will be considered elsewhere.

From the linear growth rate and radial eigenmode width it is possible to make some inferences concerning the fluctuation level in the steady state. The linear growth rate and mode width are obtained from solution of the linear eigenmode equation, which is derived by linearizing and combining the three fluid equations, Eqs. (1):

$$\rho_s^2\frac{d^2}{dx^2}\hat{\phi}_k + \left(-k^2\Omega^2 + \frac{1-\Omega}{[\Omega+(1-\eta_i)/\tau]} + \frac{(x^2/\rho_s^2)(L_n^2/L_s^2)}{\Omega^2}\right)\hat{\phi}_k = 0 \qquad (2)$$

where Fourier transformation in time and the periodic y variable has been performed, $\Omega \equiv \omega/\omega_*$, and the adiabatic coupling term has been neglected in the linear theory. The solution of Eq. (2) is given in terms of Hermite polynomials, $\hat{\phi}_k = \exp(-x^2/\rho_s^2 x_s)$

$H_\ell[(ix^2/\rho_s^2 x_s)^{1/2}]$ where ℓ, the radial eigenmode number, is an integer and $x_s \equiv \Omega L_s/L_n$. The mode width is $\Delta_k = \rho_s x_s^{1/2}$ and the eigenmode frequency Ω is given by solution of the linear dispersion relation

$$\Omega^2(k^2\rho_s^2 + 1) + \Omega\left(k^2\rho_s^2\frac{(1+\eta_i)}{\tau} - 1 + i\,(2\ell+1)\frac{L_n}{L_s}\right) + i(2\ell+1)(1+\eta_i)\frac{L_n}{L_s\tau} = 0\,. \tag{3}$$

The two roots of this dispersion relation correspond to shear damped Pearlstein-Berk drift waves and the unstable η_i mode. The exact root of the η_i-mode is

$$\Omega = \frac{A}{2(b+1)}\left(1 - \sqrt{1 - \frac{i4(b+1)(2\ell+1)(1+\eta_i)L_n}{L_s\tau A^2}}\right), \tag{4}$$

where $A = 1 - b(1+\eta_i)/\tau - i(2\ell+1)L_n/L_s$ and $b = k^2\rho_s^2$. An approximate idea of how $\mathrm{Im}\Omega$ varies with ℓ can be obtained by Taylor-expanding the radical for small ℓ. Since b and L_n/L_s are small, the two lowest orders in the expansion yield

$$\mathrm{Im}\Omega \cong \frac{(2\ell+1)(1+\eta_i)\frac{L_n}{L_s\tau}}{1 + (2\ell+1)^2\frac{L_n^2}{L_s^2}} \tag{5}$$

where $b(1+\eta_i)/\tau$ has been neglected compared with unity. For small ℓ, Eq. (5) gives $\mathrm{Im}\Omega \cong (2\ell+1)(1+\eta_i)L_n/L_s\,\tau$, which is the formula typically cited. For $\ell > 0$, Im Ω increases linearly for small ℓ and turns over for higher ℓ (at $2\ell+1 = L_s/L_n$). This is consistent with the behavior of the exact root, whose variation as a function of ℓ is illustrated in Fig. 3. From Eq. (5), the mode width is

$$\Delta_k = \rho_s \frac{\left(\frac{(2\ell+1)(1+\eta_i)}{\tau}\right)^{1/2}}{\left(1 + \frac{(2\ell+1)^2 L_n^2}{L_s^2}\right)^{1/2}}, \qquad (6)$$

which for small ℓ increases with ℓ as $\ell^{1/2}$. The fact that both growth rate and mode width increase with ℓ implies that turbulent diffusion is a strongly increasing function of ℓ. This situation differs from that encountered with drift waves where higher order eigenmodes are less localized but are also less strongly driven. In the drift wave case, turbulent diffusivities actually decrease with increasing eigenmode number. For the η_i mode, the increase of growth rate with increasing radial eigenmode number can be attributed to its sonic character. The growth rate is given approximately by Im $\Omega \cong k_{\|} C_s (1+\eta_i)^{1/2}$ where $k_{\|} \cong \Delta_k k_y / L_s$. Thus, larger modewidth corresponds to larger parallel wavenumber and stronger growth. In drift waves, by contrast, sound waves mediate the coupling to the dissipation (ion Landau damping) so that broader radial modes experience stronger dissipation. It is worth noting that η_e modes[12] are similar to η_i modes in regards to higher order eigenmode properties. Because the mathematical structure of η_e modes is equivalent to that of η_i modes with the roles of electrons and ions reversed, η_e modes with larger eigenmode number will also be more strongly driven. However, η_e modes, like η_i modes, are subject to Landau damping (electron Landau damping in the case of η_e modes). This restricts the number of unstable higher order eigenmodes and bounds the radial fluctuation scale.

Numerical solution of linearized kinetic equations for the η_i instability indicates that the role and effect of higher order radial eigenmodes is essentially the same in kinetic theory as in fluid theory with the range in ℓ of unstable modes restricted. The kinetic eigenvalue equation is

$$\left(\frac{d^2}{dx^2} + \frac{A(x,\Omega)}{D(x,\Omega)}\right)\phi(x) = 0 \qquad (7)$$

where

$$A(x,\Omega) = (1+\tau)\Omega\frac{\eta_i}{\tau} + \left\{\left(1+\tau\,\Omega\frac{\eta_i}{\tau}\right)\Gamma_o - \frac{\eta_i}{2}[\Gamma_o - 2b(\Gamma_1-\Gamma_o)]\right\}\zeta_i Z(\zeta_i) +$$
$$\eta_i\Gamma_o\zeta_i^2[1+\zeta_i Z(\zeta_i)],$$

$$D(x,\Omega) = \left\{\left(\frac{\eta_i}{\tau}\Omega + \tau^{-1}(1-\eta_i/2)\right)\zeta_i Z(\zeta_i) + \eta_i\tau^{-1}\zeta_i^2\,[1+\zeta_i Z(\zeta_i)]\right\}(\Gamma_o-\Gamma_1)$$
$$+ \eta_i\,\tau^{-1}\,\zeta_i Z(\zeta_i)\,[\Gamma_o - 2b(\Gamma_o - \Gamma_1)]\,,$$

and $\Omega = \omega/\omega_{*T}$, $\omega_{*T} = (cT_e/eB)k_y/L_T$, $\omega/\omega_* = (\omega/\omega_{*T})\eta_i/\tau = \Omega\eta_i/\tau$, $\Gamma_j = \Gamma_j(b) = I_j(b)\exp(-b)$ [$I_j(b)$ is the modified Bessel function], $b = (k_y\rho_i)^2$, $\rho_i = V_{ti}/\omega_{ci}$, $\rho_s^2 = \tau\rho_i^2$, $\zeta_i = \omega/(k_\parallel V_{ti}\sqrt{2})$, and x is in units of ρ_s ($x/\rho_s \rightarrow x$). Kinetic solutions show that the mode width is a function of the eigenmode number ℓ with only weak dependence on other parameters such as L_s/L_T and η_i. As in the fluid case, the kinetic growth rate increases for small ℓ, peaks and then decreases until it becomes negative at higher values of ℓ. The values of ℓ at which the growth rate peaks and becomes negative are lower in kinetic theory than in fluid theory. Numerical solutions show that for $L_s/L_n = 11.2$ and $\eta_i = 10$, the growth rate for $1 \le \ell \le 8$ remains above that of the $\ell = 0$ mode with the growth rate peaking at $\ell = 3$. Similarly, for $L_s/L_n = 28$ and $\eta_i = 4$, the growth rate for $1 \le \ell \le 9$ remains above the $\ell = 0$ growth rate with a peak at $\ell = 3$. In general, for weaker shear, a larger number of eigenmodes are unstable.

The scaling of the growth rate with respect to shear changes markedly for higher eigenmode numbers. For $\ell = 0$, the growth rate decreases for decreasing shear strength while for higher ℓ, the opposite is holds. The ℓ value at which the shear scaling changes is found to increase for decreasing η_i. This behavior is summarized in Fig. 4 which shows the growth rate as a function of ℓ for various values of L_s/L_n. From the numerical solutions of the kinetic equations, it can be concluded that for values of η_i consistent with experiment and for realistic shear, consideration of the first few nonzero radial eigenmodes is sufficient to determine the effect of extended fluctuations on transport. Conclusions drawn from fluid theory should also be valid for these low mode numbers.

The results of linear theory showing larger growth rates and broader mode widths provide strong indication that fluctuation levels and transport coefficients increase

when proper account is taken of extended fluctuation structure. In the next section, a nonlinear analysis is presented in order to establish this assertion.

IV. Nonlinear Eigenmode analysis

Mixing length theory has been shown to give qualitatively correct fluctuation levels and transport coefficients for η_i turbulence[4]. However, it is important to verify that estimates obtained from mixing length analysis are consistent with more rigorous nonlinear treatments which introduce no a priori scale assumptions. To this end we consider a nonlinear analysis[8,13] of the renormalized equations for ion temperature gradient driven turbulence. The full equations are derived in Ref. 13. These equations are

$$\frac{\partial}{\partial t}(1 - \nabla_\perp^2)\,\hat{\phi}_k + i\omega_{*e}\left(1 + \frac{1+\eta_i}{\tau}\nabla_\perp^2\right)\hat{\phi}_k + i\,k_\parallel \hat{v}_\parallel = -\frac{\partial}{\partial x}\mu_k \frac{\partial}{\partial x}\nabla_\perp^2 \hat{\phi}_k + \frac{\partial}{\partial x}\beta_k \frac{\partial}{\partial x}\hat{\phi}_k$$

$$\frac{\partial}{\partial t}\hat{v}_{\parallel k} + \mu\, k_\parallel^2 \hat{v}_{\parallel k} + i\,k_\parallel \hat{\phi}_k + i\,k_\parallel \hat{p}_k = \frac{\partial}{\partial x} D_k \frac{\partial}{\partial x}\hat{v}_{\parallel k}$$

$$\frac{\partial \hat{p}_k}{\partial t} + i\omega_* \frac{1+\eta_i}{\tau}\hat{\phi}_k + i\,\Upsilon\, k_\parallel \hat{v}_{\parallel k} = \frac{\partial}{\partial x} D_k \frac{\partial}{\partial x}\hat{p}_k \qquad (8)$$

where $\nabla_\perp^2 = \partial^2/\partial x^2 - k_y^2$, $\mu_k = \Sigma_{k'} [k_y^2/(k_y + k_y')^2]\, k_y'^2 |\, \hat{\phi}_{k'}\,|^2 / \Delta\omega_{k+k'}$ is the eddy diffusivity, $\beta_k = \Sigma_{k'} [k_y^2/(k_y + k_y')^2]\, k_y'^2 |\, \nabla_\perp \hat{\phi}_{k'}\,|^2 / \Delta\omega_{k+k'}$ is the turbulent back-reaction to eddy diffusivity, $D_k = \Sigma_{k'} k'^2 |\hat{\phi}_{k'}|^2 / \Delta\omega_{k+k'}$ is the turbulent diffusivity of pressure and velocity, and $\Delta\omega_{k+k'}$ is the nonlinear eddy decay rate[4]. In this renormalization, both driven vorticity and driven potential are retained, with the effects of the later being expressed in terms of the former. Consequently, the eddy diffusivity

contains a diffusivity of vorticity which is equal to D_k and a contribution from the driven potential. These two contributions combine to produce the form of μ_k given above. Approximately, $\mu_k \cong (k_y^2 / \langle k_y^2 \rangle_{rms}) D_k$, so that μ_k is less than D_k for fluctuations which are driven at low k (and cascade to higher wavenumbers where dissipation damps the fluctuation energy). In addition to the nonlinear effects represented in D_k, μ_k, and β_k, Eqs. (8) contain the physics of the pressure gradient source and saturation by parallel viscosity which models Landau damping.

A nonlinear eigenmode equation is obtained be combining Eqs. (8). The diffusivities are treated as eigenvalues to be determined by solution of the eigenmode equation. The mode width of the eigenfunction obtained from the solution is the nonlinear radial fluctuation scale. At saturation ($\gamma = 0$), the eigenmode equation is

$$\frac{\partial^2 \hat{\psi}_k}{\partial z^2} = - \frac{N^2}{9} \left(\frac{1 - |z|^{2/3} + iBS|z|^{2/3} - iMS|z|^{4/3}}{1 + iSN|z|^{2/3}} \right) \hat{\psi}_k \qquad (9)$$

where $\hat{\psi}_k = [\, 1 - i|z|^{2/3} / NS \,] \hat{\phi}_k$, $z = k_x^3 \rho_s^3 \kappa^{3/2}$, $\kappa = (1+\eta_i)/\tau$, $S = L_n/L_s$, $N = D_k / (\kappa^2 \omega_* \rho_s^2 S)$, $M = \mu_k / (\kappa^2 \omega_* \rho_s^2 S)$, $B = \beta_k |z|^{2/3} / (\kappa \omega_* \rho_s^2 S)$, and k_x is the Fourier transform variable conjugate to x, i.e., $\partial/\partial x \rightarrow ik_x$, $x \rightarrow i\partial/\partial k_x$. The normalizations of the eigenvalues N, M, and B are obtained from the $\ell = 0$ mixing length scaling of turbulent diffision with respect to the parameters κ and S (Ref.4). The mode width Δz is normalized so that $\Delta z = 1$ is the linear eigenmode width. The back-reaction β_k has an additional scaling with the square of the normalized mode width Δz due to its $|\nabla_\perp \hat{\phi}|^2$ dependence.

The eigenmode equation, Eq. (9), is solved numerically for a single eigenvalue N where B/N and M/N are taken as constants of order unity or smaller. Although the back-reaction is frequently neglected in theoretical calculations, the relations following Eqs. (7) clearly show that it is of the order of $\mu_k/\Delta z^2$. As stated previously, μ_k is a significant fraction of D_k. Accordingly B is retained in the numerical solution of Eq. (9). In choosing the ratio B/N, the normalized mode width present in β_k is assumed to be of order unity for $\ell = 0$. This assumption is verified a posteriori from the numerical

solution. It is found that above some critical eigenmode number, the turning point is dominated by the balance of the B and M terms in the potential, and does not involve the term $1-|z|^{2/3}$. Since the latter term is essential to the η_i branch of the dispersion relation, fluctuations in which the B and M terms dominate are not nonlinear η_i modes. Hence, the results of the nonlinear eigenmode calculation are not relevant above this critical eigenmode number. The critical eigenmode number increases with increasing shear. For $L_s/L_n = 25$, it is found to be $\ell=4$. Since kinetic effects restrict the range of eigenmode numbers in any case, the numerical results are given only for these lower eigenmode numbers.

The results of the numerical solution are summarized in Fig. 5. The nonlinear mode width for $\ell = 0$ is found to be comparable to the linear eigenmode width. The diffusivities are expressed as the mixing length diffusivity for $\ell = 0$ [$D_k = \omega_* \rho_s^2 (1+\eta_i)^2 L_n/L_s \tau^2$, (Ref. 4)] times a multiplicative factor. For $\ell = 0$, the factor is 3.26. For $\ell = 1$, the factor increases to 20; for $\ell = 2$, it is 40. The mode width Δz is seen to decrease as ℓ increases. Since $\Delta z \propto k_x^3$ and k_x is the Fourier transform variable conjugate to x, a decrease in Δz signifies an increase in the mode width Δx as ℓ increases. Nonlinear eigenmode analysis clearly demonstrates that a marked increase in fluctuation level and transport occurs for the less localized fluctuations corresponding to higher order nonlinear eigenmodes.

The solution of the nonlinear eigenmode equation shows that the nonlinear mode width is in good agreement the linear mode width. Moreover, the nonlinear diffusivity for $\ell = 0$ is well approximated by the mixing length diffusivity. It is therefore useful and desirable to calculate mixing length estimates of fluctuation amplitudes and diffusivities for $\ell > 0$. Mixing length estimates of fluctuation amplitudes at saturation are based on the notion that the cascade can be approximated by a nonlinear mixing of pressure inputed by the gradient source over a characteristic fluctuation scale in the gradient direction. In its simplest form, mixing length theory balances the linear growth rate with turbulent diffusion over the linear mode width. In the simplest renormalized treatment of the nonlinear equations, the convective nonlinearity is everywhere replaced by a radial diffusion: $\int dy\, (\hat{b} \times \nabla \hat{\phi} \cdot \nabla)\, \exp(iky) \rightarrow \partial/\partial x\, D_k\, \partial/\partial x$ where the diffusion coefficient D_k is the same given immediately following Eqs (8). The mixing length balance then implies that $\mathrm{Im}\, \Omega_k = D_k/\Delta_k^2$. From the linear growth rate and mode width, we infer that

$$D_k = \frac{\omega_* \rho_s^2 (2\ell+1)^2 (1+\eta_i)^2 \frac{L_n}{L_s \tau^2}}{[\,1 + (2\ell+1)^2 \frac{L_n^2}{L_s^2}\,]^2} \qquad (10)$$

Setting $\ell = 0$, recovers previous results[4]. Note, however, that in going from $\ell = 0$ to $\ell = 1$ there is nearly an order of magnitude increase in the diffusion coefficient with further increases for higher values of the radial eigenmode number.

It is also possible to obtain a mixing length diffusivity from kinetic theory by using the growth rates and mode widths obtained from shooting code solutions. For comparison, Fig. 6 shows the diffusivities of kinetic theory, fluid theory [using the more exact $\mathrm{Im}\Omega$ obtained from Eq. (4) rather than the approximate one given by Eq. (5)], and the nonlinear theory as a function of ℓ for $L_s/L_n = 28$ and η_i=4. It is seen that all theories agree very well for the low values of ℓ considered. For higher values of the eigenmode number, the agreement becomes worse, for the reasons which have already been discussed at some length.

The large anomalous ion thermal conductivity resulting from excitation of even the lowest ($\ell \neq 0$) radial eigenmodes strongly enforces proximity to marginal stability through rapid relaxation of unstable temperature profiles. Note that the strong ℓ dependence effectively allows χ_i to remain large, even in regions where the ion temperature is lower. It is also interesting to speculate on scaling of the diffusion coefficient implied in Eq. (10). For $\ell = 0$, $D_k \propto L_n/L_s$; however for higher values of ℓ, the denominator of Eq. (10) becomes important and can alter the simple scaling inferred from the numerator. This is underscored by evaluating D_k at the mode number giving maximum diffusion, i.e., $(2\ell+1) = L_s/L_n$. In that case $D_k = 0.25\omega_* \rho_s^2 (1+\eta_i) L_s/L_n \tau^2$. Note that the L_n/L_s scaling of the $\ell = 0$ theory is altered to become an L_s/L_n scaling. While the value of ℓ which yields this scaling is probably too high for instability (determined from kinetic theory) when the shear is strong, this exercize nevertheless indicates that scalings in the weak shear limit are altered. A scaling of D_k with L_s to some positive power is consistent with the kinetic growth rate [Fig. (4)], which shows stronger excitation for decreasing shear strength and a larger range of unstable eigenmodes .

The fluctuation level consistent with mixing length diffusion, Eq. (10), is readily found from the formula for D_k, assuming that the eddy decay rate $\Delta\omega_{k+k'}$ is approximately the diffusion time D_k/Δ_k^2. This yields

$$\frac{\hat{n}}{n_0} = \left|\frac{e\phi}{T_e}\right| \cong \frac{\rho_s}{L_s}\left(\frac{(2\ell+1)(1+\eta_i)/\tau}{[1+(2\ell+1)^2\frac{L_n^2}{L_s^2}]}\right)^{3/2}, \qquad (11)$$

once again showing that a strong increase occurs in going from $\ell = 0$ to $\ell = 1$. This result is consistent with the conclusions of the nonlinear eigenmode calculation, particularly in showing significant increases in the diffusivities for higher order radial mode structure.

V. Conclusions

Higher order radial eigenmodes are more strongly driven than the $\ell = 0$ eigenmode typically used to characterize the radial mode structure of ion temperature gradient driven turbulence. The results of particle simulations show that these more extended fluctuations characterize the potential in the saturated state. From nonlinear eigenmode analysis of the renormalized equations, it is shown that consideration of these eigenmodes leads to diffusivities and fluctuation levels which are typically much larger than those obtained with the lowest eigenmode number structure. Mixing length estimates of the diffusivity based on both kinetic and fluid theories are also calculated and shown to be in good agreement with the diffusivity of the renormalized nonlinear eigenmode equation. The scaling of the diffusivity with respect to shear is also considered. For weak shear, qualitatively consistent scalings from linear theory and mixing length estimates suggest that D increases with L_s. The large value of thermal conductivity inferred from these considerations suggests that in practice, η_i could not greatly exceed the instability threshold and that the system would be tied dynamically to marginally stable η_i profiles in NBI and ICRF heated plasmas. Moreover, the enhancement of χ_i allows the domain of quasi-

marginality to extend to regions of colder plasma. Finally, we speculate that η_i-mode turbulence may constitute a 'marginal stability' link between the hot core and cooler edge plasma. Such links are thought to be the dynamical underpinning of profile consistency[14] phenomena. Given these conclusions, a nonlinear kinetic calculation of ion temperature gradient driven turbulence is desirable.

Acknowledgments

We acknowledge useful discussions with J.F. Drake. We also acknowledge stimulating discussions with R.J. Goldston and Y. Takase on the subject of dynamical marginal stability and the links between the edge and core plasma. This work was supported by the U.S. Department of Energy contract #DE-FG05-80ET-53088.

References

1. R.J. Groebner, W.W. Pfeiffer, F.P. Blau, and K.H. Burrell, Nucl. Fusion **26**, 543 (1986).
2. S.M. Wolfe and M. Greenwald, Nucl Fusion **26**, 329 (1986).
3. D.L Brower, W.A. Peebles, S.K. Kim, N.C. Luhmann, Jr., W.M Tang, and P.E. Phillips, Phys.Rev. Lett. **59**, 49 (1987).
4. G.S. Lee and P.H. Diamond, Phys. Fluids **29**, 3291 (1987).
5. B. Coppi, M.N. Rosenbluth, and R.Z. Sagdeev, Phys. Fluids **10**, 582 (1967).
6. R.J. Goldston, et al., in Controlled Fusion and Plasma Physics, S. Methfessel, ed., (European Physical Society, Madrid, 1987) p. 140.
7. J.N. Leboeuf, D.R. Thayer, and P.H. Diamond, Bull. Am. Phys. Soc. **31**, 1404 (1986).
8. L. Garcia, B.A. Carreras, and P.H. Diamond, Phys. Fluids.**30**, 1388 (1987).
9. W.W. Lee, W.M. Tang, and H. Okuda, Phys. Fluids **23**, 2007 (1980); H. Okuda, J.M. Dawson, A.T. Lin, and C.C. Lin, Phys. Fluids **21**, 478 (1978).
10. P.N. Guzdar, Liu Chen, W.M. Tang, and P.H. Rutherford, Phys. Fluids **26**, 673 (1983).
11. P.W. Terry, W. Anderson, and W. Horton, Nucl. Fusion **22**, 487 (1982).
12. P.N. Guzdar, C.S. Liu, J.Q. Dong, and Y.C. Lee, Phys. Rev. Lett. **57**, 2818 (1987).
13. N. Mattor and P.H. Diamond, Phys. Fluids (in press).
14. B. Coppi, Comments Plasma Phys. Controlled Fusion **5**, 261 (1980).

Figure Captions

Fig. 1. Particle simulation results for one single even parity mode unstable with $k_\perp \rho_s = 0.3$, $\eta_i = 4$, $L_s/L_n = 28$, and $T_e = T_i$ showing the real and imaginary parts of the potential fluctuation [solid and broken lines respectively]; a.) Snapshot of the spatial structure of the potential fluctuation in the simulation at saturation; b.) Fundamental even eigenmode from linear theory (radial mode number $\ell = 0$); c.) Eigenmode from linear theory with radial mode number $\ell = 2$.

Fig. 2. Particle simulation results for one single odd parity mode unstable with $k_\perp \rho_s = 0.3$, $\eta_i = 10$, $L_s/L_n = 11.2$, and $T_e = T_i$ showing the real and imaginary parts of the potential fluctuation [solid and broken lines respectively]; a.) Snapshot of the spatial structure of the potential fluctuation at saturation ($\omega_* t = 9.0$); b.) Spatial structure of the fluctuation with $\omega = -1.42\omega_*$ obtained by interferometry from the simulation data; c.) Spatial structure of the fluctuation with $\omega = -1.94\omega_*$ by interferometry; d.) Eigenmode from linear theory with $\ell = 1$ and $\omega = -0.995\omega_*$; e.) Eigenmode from linear theory with $\ell = 3$ and $\omega = -1.61\omega_*$; f.) Eigenmode from linear theory with $\ell = 5$ and $\omega = -2.1\omega_*$.

Fig. 3. Growth rate as a function of ℓ from solution of the fluid equations [Eq. (4)] with $L_s/L_n = 15$, $k_\perp \rho_s = 0.07$, and $T_e/T_i = 2$.

Fig. 4. Growth rate from numerical solution of the kinetic equations as a function of ℓ for three values of the shear, $L_s/L_n = 10$, 25, and 50, and $\eta_i = 4.0$. Growth rate decreases with decreasing shear strength for $\ell = 0$ while for $\ell > 0$ it increases for decreasing shear strength.

Fig. 5. Nonlinear diffusivity D_k normalized by $\omega_* \rho_s^2 (1+\eta_i)^2 L_n / L_s \tau^2$ as a function of ℓ obtained from numerical solution of the renormalized eigenmode equation for $L_s/L_n = 15$.

Fig. 6. Comparison of mixing length diffusivities obtained from the growth rates and mode widths of kinetic and fluid theories with the diffusivity obtained from numerical solution of the renormalized eigenmode equation for $L_s/L_n = 28$, $\eta_i = 4$, and $T_e = T_i$

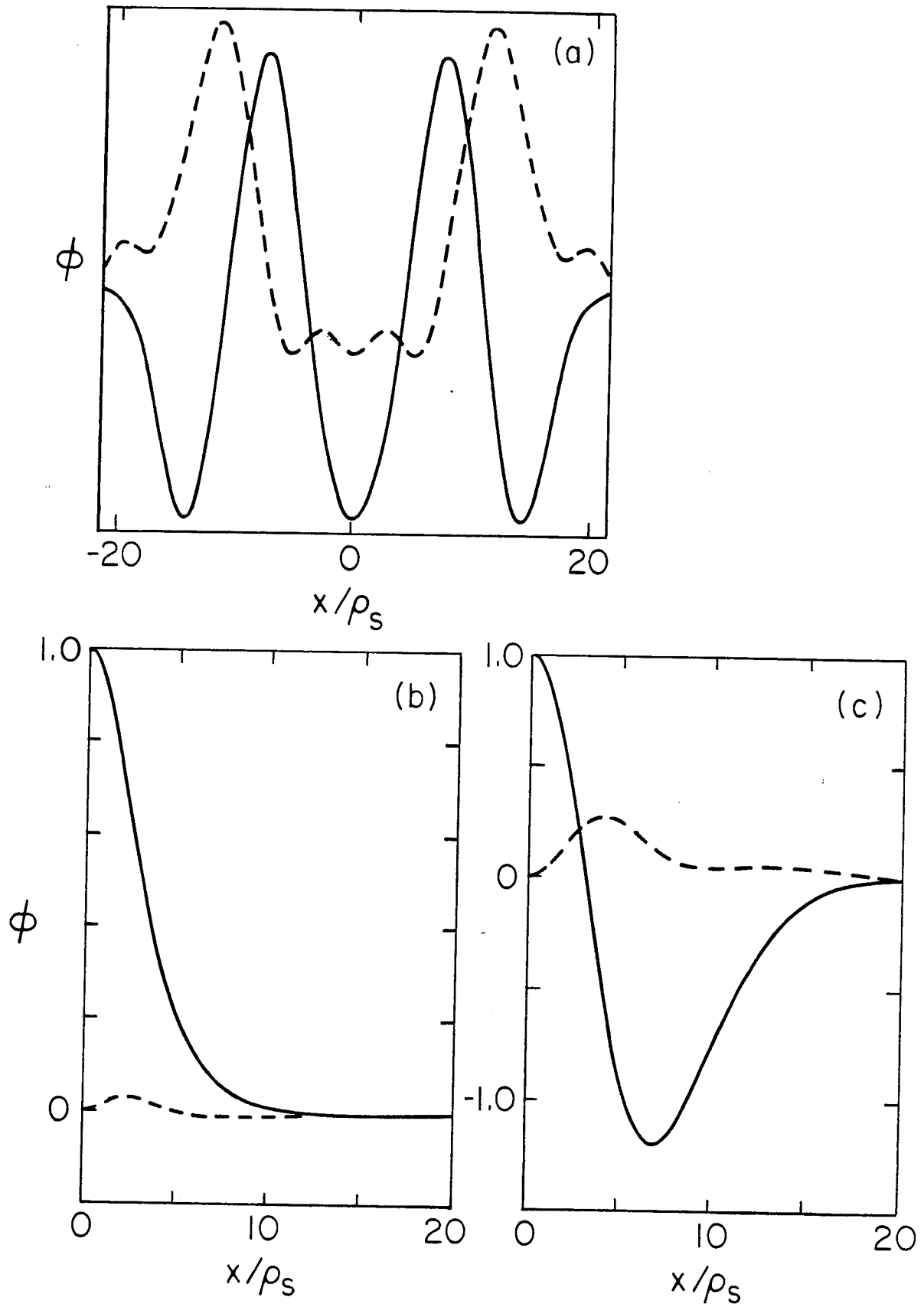

Fig. 1

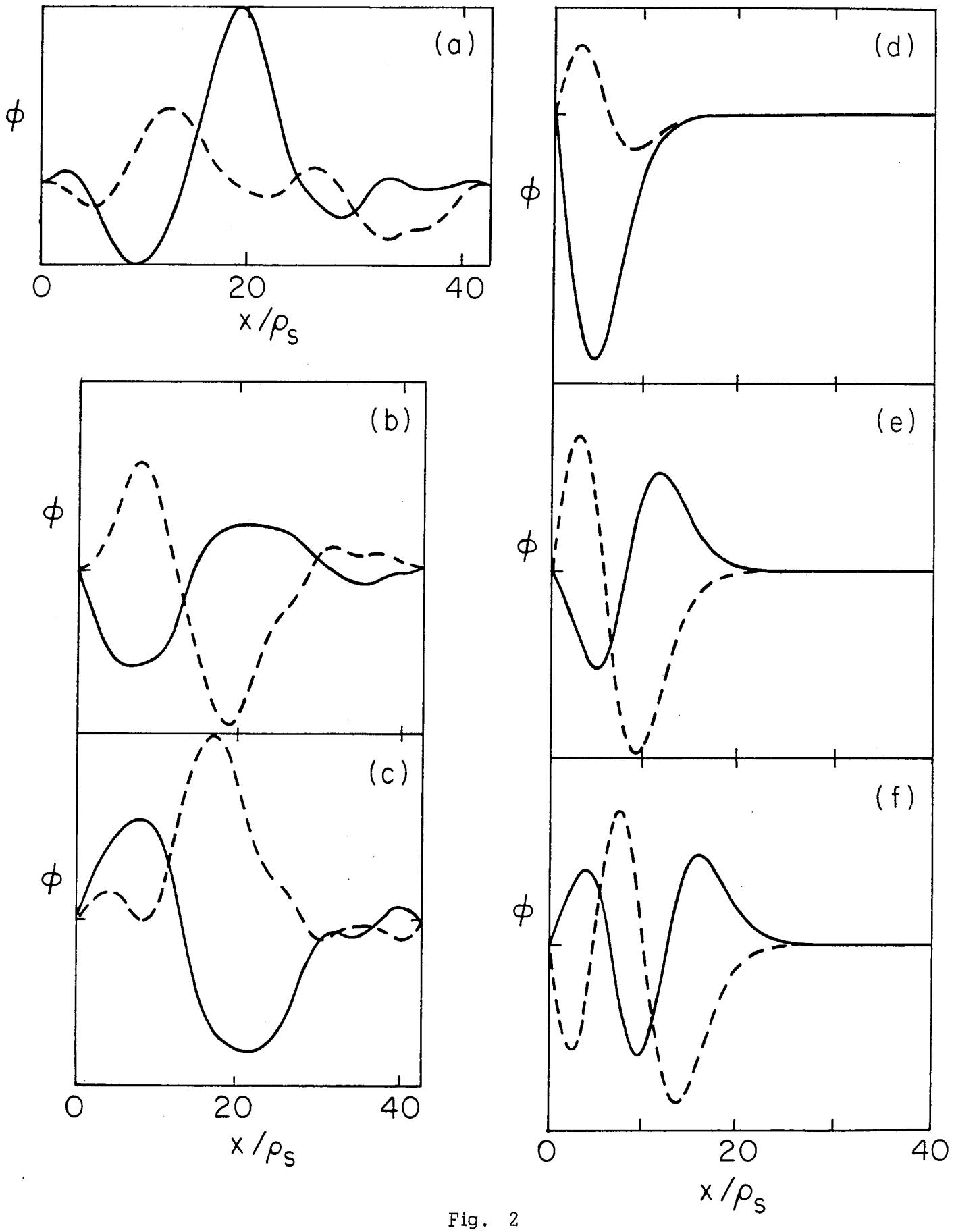

Fig. 2

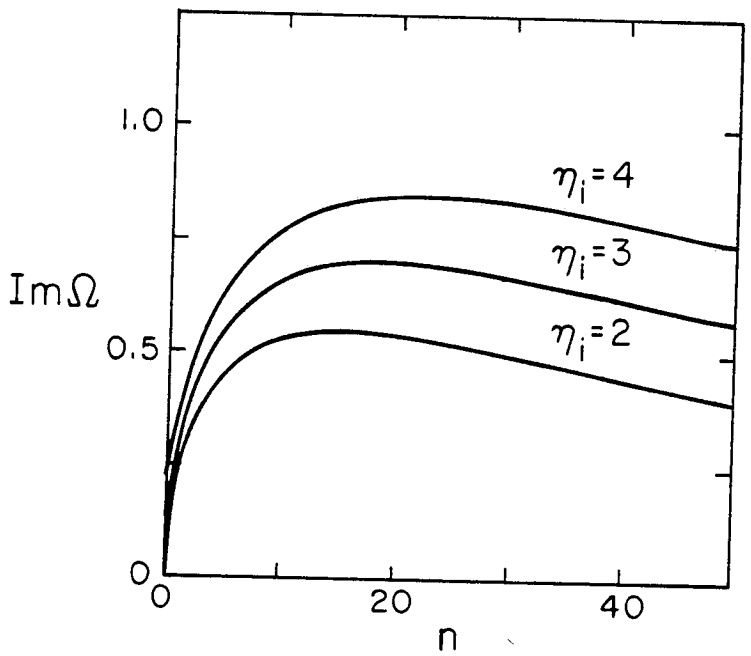

Fig. 3

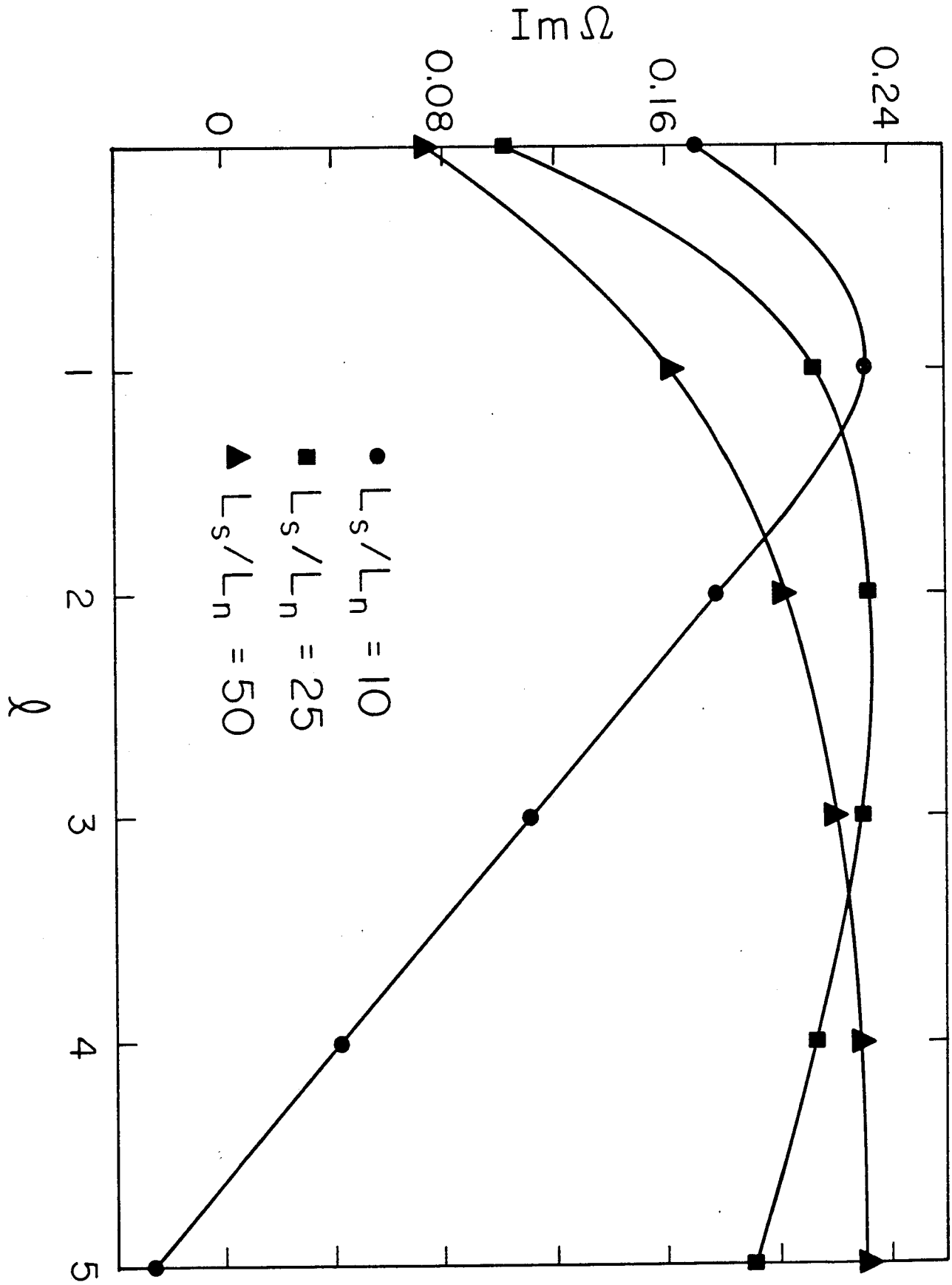

Fig. 4

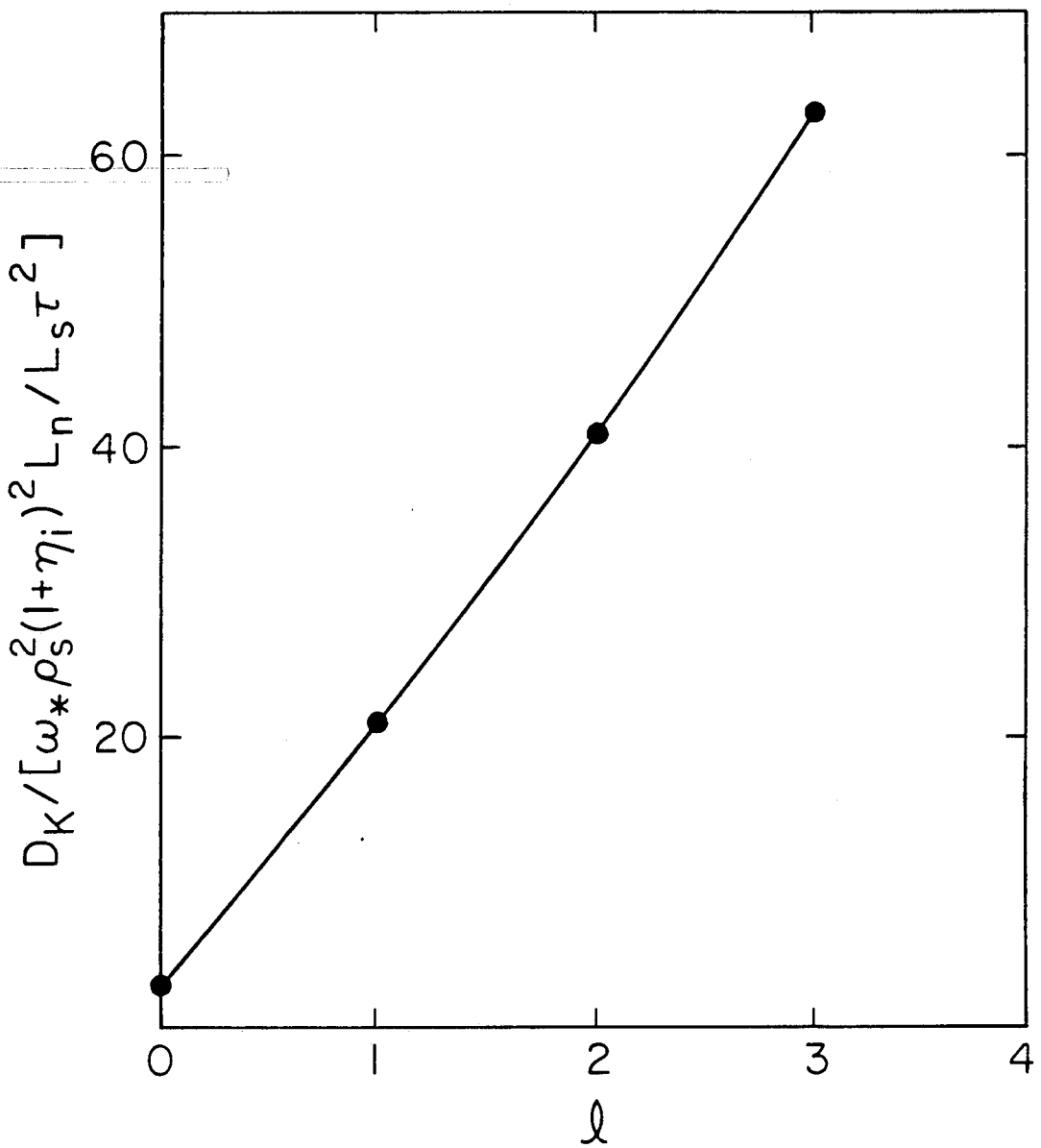

Fig. 5

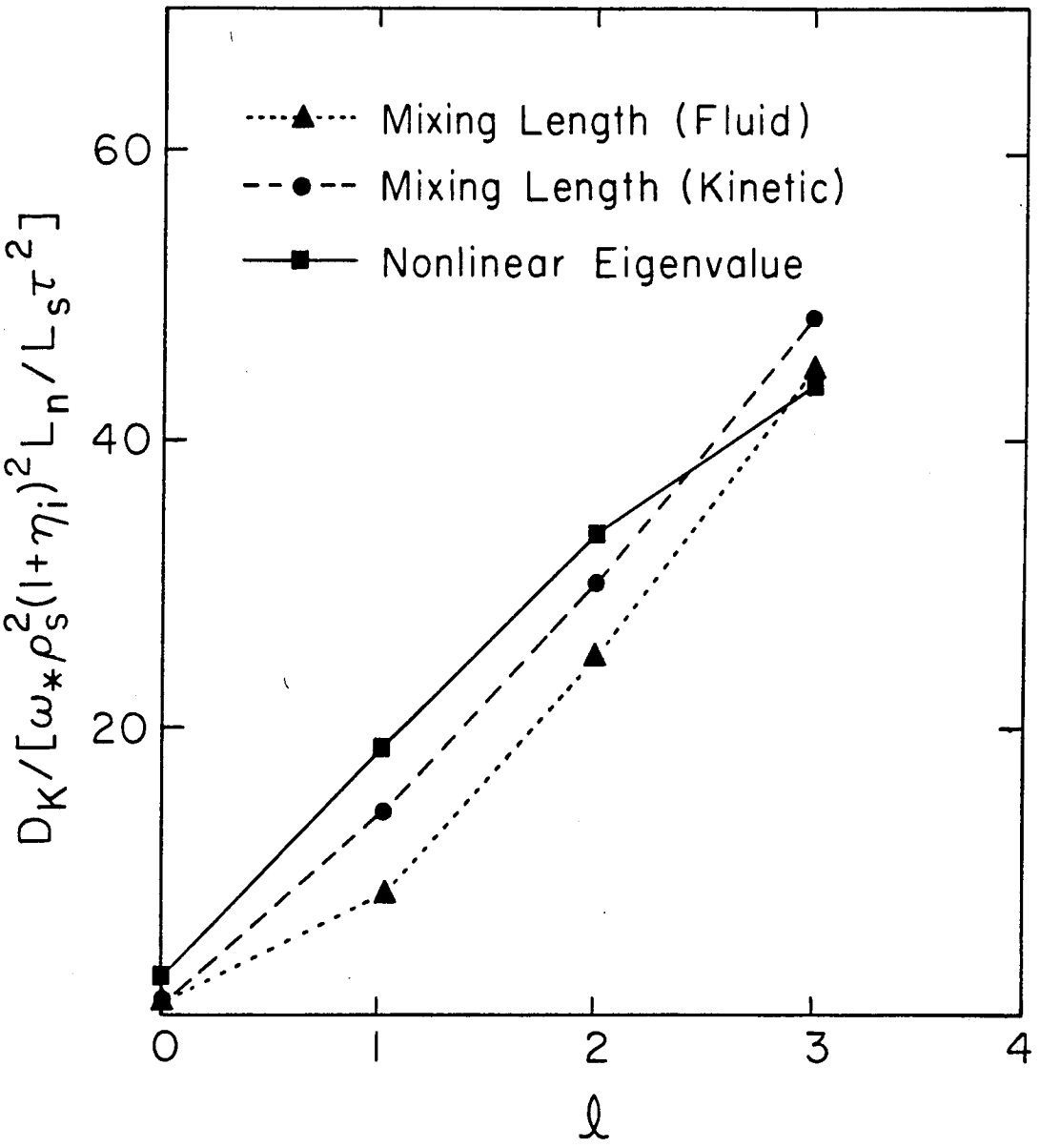
Mixing Length (Fluid)
Mixing Length (Kinetic)
Nonlinear Eigenvalue
60
40
20
0
1
2
3
4
ℓ
$D_K/[\omega_* \rho_s^2 (1+\eta_i)^2 L_n / L_s \tau^2]$

Fig. 6